

Can new synthetic stellar atmospheres explain the red halos of Blue Compact Galaxies?

Giovanni Lugaro

Bachelor Thesis, 10 points
Supervised by Erik Zackrisson

October 6, 2004

Abstract

Blue Compact Galaxies (BCGs) are objects still not completely understood. Comparing relatively close BCGs to spectral evolutionary models (SEMs), we see that different stellar populations are present in the centre and in the halo of a BCG. The colour of the central burst, where the star formation rate is high, agrees very well with SEMs computed for a young metal-poor stellar population. Instead, the colour of the halo does not agree with SEMs, showing a redder colour than expected. The halo may be in principle be interpreted as an old metal-rich stellar population, since it lies close to the metal-rich evolutionary track, but this remains controversial. Another possible explanation for the red excess compared to model predictions is the use of synthetic stellar atmospheres which may be of dubious quality. Programming in Matlab, we computed the differences in the colours resulting in SEMs by using old (Lejeune et al. 1998) or new (MARCS, Gustafsson et al. 2004) synthetic stellar atmosphere models. We found large differences in the results between the two cases, in the direction of an improvement in the match with the observations using the new model atmospheres, but only for stars with $T \leq 4000K$ and $M \leq 0.8M_{\odot}$. These differences, hence, do not help matching the observations of the red halo because such low mass stars do not contribute much to its light. However, using the MARCS(2004) model it may be possible to explain the red halo if its initial mass function (IMF) is bottom-heavy compared to the standard Salpeter IMF.

1. Introduction

“Per ogni gabola c’è uno sgabolo”
Mauro Cirio

1.1. What are BCGs

Blue Compact Galaxies (BCGs), sometimes called HII galaxies, are characterized by globally active star formation, low chemical abundances (e.g. Searle & Sargent 1972; Marconi et al. 1994; Kunth & Östlin 2000; Masegosa et al. 1994) and relatively high HI masses (Gordon & Gottesman 1981; Thuan & Martin 1981; Staveley-Smith et al. 1992). These are properties normally associated with young galaxies and indeed there have been claims from time to time (Searle & Sargent 1972; Thuan & Izotov 1997) that some BCGs may be truly young systems. It is important to understand how they were formed and the connection with their progenitors (HI clouds, Low Surface Brightness galaxies, e.g. Bergvall et al. 1998, 2000; Mihos et al. 1997, or other gas rich dwarfs) because BCGs constitute an important link to the high redshift universe and the early epoch of galaxy formation.

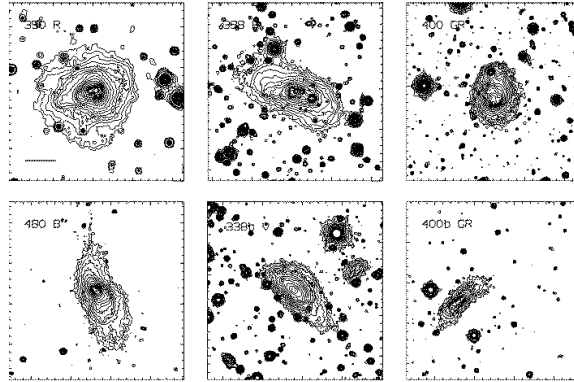


Figure 1. Optical broadband images of ESO 338-IG04 (Tol 1924-426), 338-IG04b, 350-IG38 (Haro 11), 400-G43, 400-G43b and 480-IG12. The filters, indicated after the abbreviated object name on top of the images, are in the Bessel system except those marked GR which is the r filter in the Thuan-Gunn system. A median 3×3 pixel filter was applied on the lower flux levels. The steps between the isophotes are constant on a logarithmic scale arbitrarily chosen for each galaxy such that the details are enhanced. North is up, east is to the left. The field size is $95'' \times 95''$.

1.2. Morphology

The class of BCGs is quite heterogeneous and may include objects with different histories, but there are some common properties:

- BCGs are not big galaxies and they look like irregular cluster of stars.
- The centre is very luminous and shows a blue colour, which agree very well with spectral evolutionary models (SEMs) for a young metal-poor stellar population (e.g. Bergvall & Östlin 2002). An intense activity in the centre reveals the explosive nature of BCGs. In fact, some BCGs change their luminosity with recurrent bursts (Östlin et al. 1998; Bergvall 1985; Bergvall & Olofsson 1986). Therefore BCGs are not quiet, but have high star formation rate. Besides, some BCGs show Wolf-Rayet features in their spectra and have strong Balmer emission lines and thus must contain a considerable fraction of very young stars. In summary, the central burst has a high star formation rate, which produces the blue colour of the BCG and contains a young metal-poor stellar population.
- Around the centre there is a faint halo. It is difficult to study the halo because of its low surface brightness. The colour of the halo is best-fitted with models for an old metal-rich stellar population (Bergvall & Östlin 2002), however, this colour is redder than predicted by SEMs. Also, a metal-rich halo is difficult to explain theoretically.

1.3. The youth hypothesis

From studies of the central starburst region of BCGs it is very difficult to rule out that the galaxy is young since the starburst population easily outshines even a relatively massive population of old stars. Also the fact that chemical abundances are low and homogeneous agree with the idea that BCGs are young galaxies, however the colour and the morphology of the halos do not. Moreover, near-IR photometry, which has proven to be quite powerful in deriving information about the star formation history in galaxies that are dominated by starburst, seems to support the idea that the BCGs are old (e.g. Bergvall et al. 1999; Doublier et al. 2001).

If the halo really contains an old metal-rich stellar population (as we see by comparing with SEMs), the youth hypothesis will have to be dismissed and it will be difficult to understand the evolution of BCGs. In fact, an old metal-rich halo would be very unusual since typically galaxies have halos made up of old but metal-poor stars. This feature is easy to understand because the halo metal-poor stars were formed, when the galaxy was young, in metal-poor star-forming nebulae without elements heavier than helium (population II stars). The population II stars (mainly when they were giants, or supernovae) then enriched the galactic medium with elements heavier than hydrogen or helium and the following generation of stars were thus formed in metal-rich nebulae (population I stars). Hence, for BCGs it is difficult to understand where the metals in the stars which compose the halo came from.

A possibility is that BCGs formed from a merger between two galaxies of different metallicities, one gas-rich and one gas-poor, or from infall of intergalactic clouds. This type of scenarios could represent the most plausible explanation of the observational features of these galaxies.

1.4. The problem of the halo

The halo is supposedly made up of a old metal-rich stellar population (e.g. Bergvall & Östlin 2002), but it is important to notice that the colour of the halo is redder than predicted by evolutionary path of SEMs. This reddening could be due to the fact that observations are affected from light of other nature.

Two sources can modify the colour of the light of the halo: nebular emission and dust emission.

1.4.1. Nebular emission

We do not know if the light of the halo contains a contribution from a nebular emission of ionized gas. Possible ionising sources are young stars or old hot stars, i.e. blue horizontal branch stars (BHB) or post-AGB stars (PAGB). We know that this type of contribution would be smaller for higher ages because in this case there would be less new blue stars ionising the gas. We can derive the colours of a pure HII region (i.e. assuming no stars in the halo) ionised by the stars in the central burst. The colours we obtain are $B - V \leq 0.74$ and $V - K \leq 0.17$: significantly bluer than observed (e.g. Bergvall & Östlin 2002). The correction would be marginal and would amount to 0.1 - 0.2 magnitudes. And the colour of the halo, after the correction, would become redder: in the opposite direction that we want.

1.4.2. Dust emission

If we suppose that the red colour is due to warm dust, then the dust must have a temperature of around 3500 K to match the observations. This dust temperature is too high to obtain if the dust would be heated by the central burst and if the dust would be heated in situ. Therefore one may conclude that the contribution from dust emission to the luminosity of the halo is insignificant.

2. SEMs: Spectral Evolutionary Models

The spectral evolutionary models (SEMs) used to integrate the halo colours of BCGs come from an inhouse model by Zackrisson et al. (2001), PEGASE2 (Fioc & Rocca-Volmerange 2000) and the model from Worthey (1994). In our work we use the Zackrisson et al. models, which are based on stellar evolutionary tracks calculated by the Geneva group, synthetic stellar spectra from the compilation by Lejeune et al. (1998) and a nebular component obtained from the Cloudy model (Ferland 1996). We have to remember that SEMs treat the centre and the halo separately, without any connection between them, as two different evolutions of two clusters of stars.

2.1 Inputs

The colour evolution predicted by SEMs depend on:

- the assumed initial mass function (IMF),
- the metallicity (Z),
- a parameter describing how the star formation rate (SFR) changes with time,
- the synthetic models of stellar atmospheres,
- the stellar evolutionary tracks, and
- the nebular emission model.

More sophisticated models also include metallicity evolution and gas flows.

2.1.1. IMF

The assumed initial mass function sets how many stars are formed for any value of the initial mass. The IMF is regulated by:

$$\frac{dN}{dM} \propto M^{-\alpha} \quad (1)$$

where N is the number of formed stars, M is the mass of formed stars and α is a parameter $\alpha = 1.35 - 3.35$, where $\alpha = 2.35$ correspond to the commonly adopted Salpeter slope. In SEMs we use a Salpeter slope. Varying the IMF one can modify the colour of the stellar cluster. For example, low mass stars at low ages are insignificant contributors of the emitted light, whereas at high ages they become red giants and they are needed to get any light at all. With a bottom-heavy IMF (i.e. $\alpha < 2.35$ so that more low-mass stars are formed), the colour of the stellar cluster would become redder. This may be one of the possible explanations for the redness of the halo.

2.1.2. Metallicity

The metallicity of a star represents the mass of metals (elements heavier than helium) with respect to the mass of hydrogen and helium. We compute evolutionary tracks with different metallicities: $Z = 0.05Z_{\odot}$, $Z = Z_{\odot}$ and $Z = 2Z_{\odot}$. In the PEGASE2 model (Fioc & Rocca-Volmerange 2000) the recycling of metals in a closed-box scenario have been taken into account.

2.1.3. SFR

The star formation rate describes how many stars are formed at a given time in the burst. Assuming that the SFR is constant in time leads to blue colours at high ages, as compared to a short burst. This is because for a constant star formation rate there are always young blue stars in the cluster, instead, after a short burst, the cluster get old and became redder because there are only old red stars. We can use a constant SFR or, to simulate a burst, we can use an exponential SFR, with a time constant of 1 to 14 Gyr.

2.1.4. Synthetic stellar atmospheres

Synthetic models for stellar atmospheres produce the spectrum $\Phi = f(\lambda)$ of a star from the specific temperature, surface gravity, metallicity and age. We compute the colours of the star integrating the theoretical spectrum in different windows of light. Then SEMs use this result to calculate the light of many stars (from IMF and SFR) and to compute the evolution of the stellar cluster. Until now Zackrisson et al. (2001) and PEGASE2 (Fioc & Rocca-Volmerange 2000) have used synthetic stellar atmospheres from Lejeune (1998).

2.1.5. Stellar evolutionary model

The synthetic stellar atmospheres are static, i.e. they do not change with time. The stellar evolutionary tracks, calculated by the Geneva group, regulates how the temperature, surface gravity and luminosity of a single star change with time.

2.1.6. Nebular emission model

The nebular emission model, from the Cloudy model (Ferland 1996), corrects the colour of the halo with the contribution of a nebular emission from ionized gas due to young or old hot stars i.e. BHB or PAGB stars.

3. The current work

3.1. The theory

3.1.1. The problem of SEMs

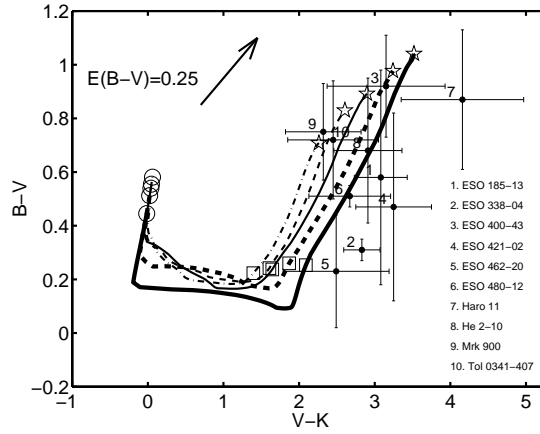


Figure 2. Halo colours (corrected for galactic extinction but not for internal extinction; 1σ errors bars) of 10 BCGs versus PEGASE2 evolutionary tracks. The evolutionary sequences include nebular emission and assume an exponentially decreasing star formation rate with an e-folding decay rate of 1 Gyr. The different lines correspond to constant metallicities of $Z=0.001$ (thin dash-dotted), 0.004 (thick dashed), 0.008 (thin solid), 0.020 (thick dashed), 0.040 (thick solid). Markers indicate ages of 0yr (circle), 1Gyr (square) and 14Gyr (pentagon). The reddening vector marked with an arrow.

Results from SEMs reproduce very well the colour of the central burst for a metal-poor stellar population, but they do not agree with the colour of the halo, which lies redward in V-K and blueward in B-V with respect to the prediction, as shown in the (V-K/B-V) graph of Figure 2. Since there does not seem to be a physical explanation (nebular or dust emission) for this discrepancy, we test the idea that perhaps SEMs are not calibrated with the correct theoretical inputs. We can test for example different choices of the IMF or new synthetic models for stellar atmospheres. The Lejeune (1998) models have been so far used in our SEMs. We now have a preview of new models of synthetic stellar atmospheres called MARCS (Model Atmospheres with a Radiative and Convective Scheme) (Gustafsson et al. 2004).

3.1.2. The target

In this work we test if the use of the new synthetic stellar atmospheres MARCS(2004) produces any changes in the evolutionary tracks and compare the colours of stars predicted using the MARCS(2004) or the Lejeune (1998) models. In the case that using the MARCS(2004) model we predict redder stars with respect to using the Lejeune model, the evolutionary paths of SEMs will be shifted redward in V-K and blueward in B-V in the (V-K,B-V) graph, in agreement with the observations of the halos.

3.2. The work

3.2.1. First step

We have a preview of the new synthetic stellar atmospheres MARCS(2004). This set of atmospheres has been computed for a grid of stars with

- three different metallicities: $Z = 0.001$, $Z = 0.020$ and $Z = 0.040$,
- surface temperature from 2500 K to 8000 K and
- logarithm of surface gravity from 2.5 to 5.0¹

The MARCS(2004) synthetic stellar atmospheres give spectra with more than 100000 flux data points, $f(\lambda)$. The program within SEMs that computes the colours of the stars from the spectra needs a spectrum with 1221 specific wavelengths. It would be very time consuming to compute the colours from a spectrum with more than 100000 data points. So we have produced a Matlab program (Appendix A) that interpolates the MARCS(2004) spectra to the specific 1221 values.

3.2.2. Second step

We computed the colours of each MARCS(2004) stellar spectrum. Then, we selected the spectra with the same temperature and the same logarithm of surface gravity between the two models (Lejeune and MARCS). With another Matlab program (Appendix B), we compared the new colours from MARCS(2004) with the old from Lejeune(1998) for the three different metallicities in the (V-K/B-V) graph. Figure 3 shows the difference in magnitudes V-K and B-V. The crosses are the data from the BCG halos (Bergvall et al. 2003). The changes produced using MARCS(2004) go toward the colours observed of the halos, but not for all the kind of stars. The largest change occurs for the stars on the right in the figure, i.e. stars with low temperature. Figure 4 shows stars for which the change from Lejeune(1998) to MARCS(2004) colours is, in all the directions, bigger than 0.2 magnitudes ($\Delta(col) \geq 0.2mag$). The largest change is for stars with $T \leq 4000K$, with the most important effect (at any metallicities) showing up for stars with: $T = 2500K$ and $log(g) = 4.0$.

3.2.3. Third step

With another Matlab program (Appendix C), we compared in detail the spectra of Lejeune(1998) and that of MARCS(2004) for stars with $T = 2500K$ and $log(g) = 4.0$. Figure 5 shows $log_{10}(\Phi_{MARCS}/\Phi_{Lejeune})$ versus $log_{10}(\lambda)$. The most important differences are in the first part of the spectrum, from about 125nm to 1000nm.

¹The geometrical extent of the photosphere in the stars varies inversely with surface gravity defined by: $g = g_{\odot} \frac{M}{R^2}$ where g_{\odot} is the surface gravity of the sun (2.738×10^4 cm/sec²) and the mass, M, and radius, R, of the star are in solar units.

From 125nm to 400nm the MARCS(2004) spectrum is up to 8 orders of magnitude more luminous than the Lejeune(1998) spectrum. From 400nm to 1000nm there are also large differences due to offsets between the peaks evident in Figure 6. We can see in Figure 7 that from 1200nm to 1750nm there is a bigger contribution from MARCS(2004) spectrum which is responsible of the reddening. We can see from the spectra computed by MARCS model (Figure 8, 9, 10 and 11) that the differences between the two spectra are probably due to TiO, CaH, Atoms, MgH, FeH, SiH and ZrO in the first part of spectra, and to water, FeH and atoms in the following part.

3.3. Conclusions

Figure 3 shows that the changes due to using the new MARCS(2004) model go in the right direction in explaining the observations, however, Figure 4 shows that this happens only for stars with low surface temperature and high surface gravity. Figure 12 shows the evolutionary tracks for stars with different masses: $M = 120, 20, 1, 0.8, 0.09 M_{\odot}$. Stars with $T \leq 4000K$ and high logarithm of surface gravity $2.5 \leq \log(g) \leq 5.0$ are stars with $M \leq .8 M_{\odot}$. From the evolutionary tracks in Figure 13, we can see that low-mass stars with $M \leq 0.8 M_{\odot}$ are the less luminous. Thus these stars do not contribute much to the light of the halo and the global change in the SEM tracks will be insignificant. Therefore, the preview of MARCS(2004) synthetic atmospheres do not explain the red halos of BCGs. A future working test will be to introduce a very unusual IMF producing many low-mass stars.

References

- Bergvall, N., Marquart, T., Persson, C., Zackrisson, E., & Östlin, G., proceedings of the conference Multiwavelength Mapping of Galaxy Formation and Evolution, Venezia, Italy, October 13-16, 2003, in press;
 Bergvall, N., & Östlin, G. 2002, A&A, 390, 891;
 Bergvall, N. 1985, A&A, 146, 269;
 Bergvall, N., & Olofsson, K. 1986, A&AS, 64, 469;
 Bergvall, N., Östlin, G., Masegosa, J., & Zackrisson, E. 1999, Ap&SS, 269/270, 625;
 Doublier, V., Caulet, A., & Comte, G. 2001, A&A, 367, 33;
 Ferland, G. J. 1996, "HAZY, a brief introduction to Cloudy", University of Kentucky, Department of Physics and Astronomy Internal Report;
 Fioc, M., & Rocca-Volmerange, B. 2000 [astro-ph/9912179];
 Gordon, D., & Gottesman, S. T. 1981, AJ, 86, 161;
 Gustafsson, B., et al. (2004), in preparation;
 Kunth, D., & Östlin, G. 2000, A&ARv, 10, 1;
 Lejeune, T., Cuisinier, F., & Buser, R. 1998, A&AS, 130, 65L;
 Marconi, G., Matteucci, F., & Tosi, M. 1994, MNRAS, 270, 35;
 Masegosa, J., Moles, M., & Campos-Aguilar, A. 1994, ApJ, 420, 576;
 Östlin, G., Bergvall, N., & Rönnback, J. 1998, A&A, 335, 85;
 Searle, L., & Sargent, W. L. W. 1972, ApJ, 173, 25;
 Staveley-Smith, L., Davies, R. D., & Kinman, T. D. 1992, MNRAS, 258, 334;
 Thuan, T.X., & Martin, G. E. 1981, ApJ, 247, 823;
 Worthey, G. 1994, ApJS, 95, 107;
 Zackrisson, E., Bergvall, N., Olofsson, K., & Siebert, A. 2001, A&A, 375, 814.

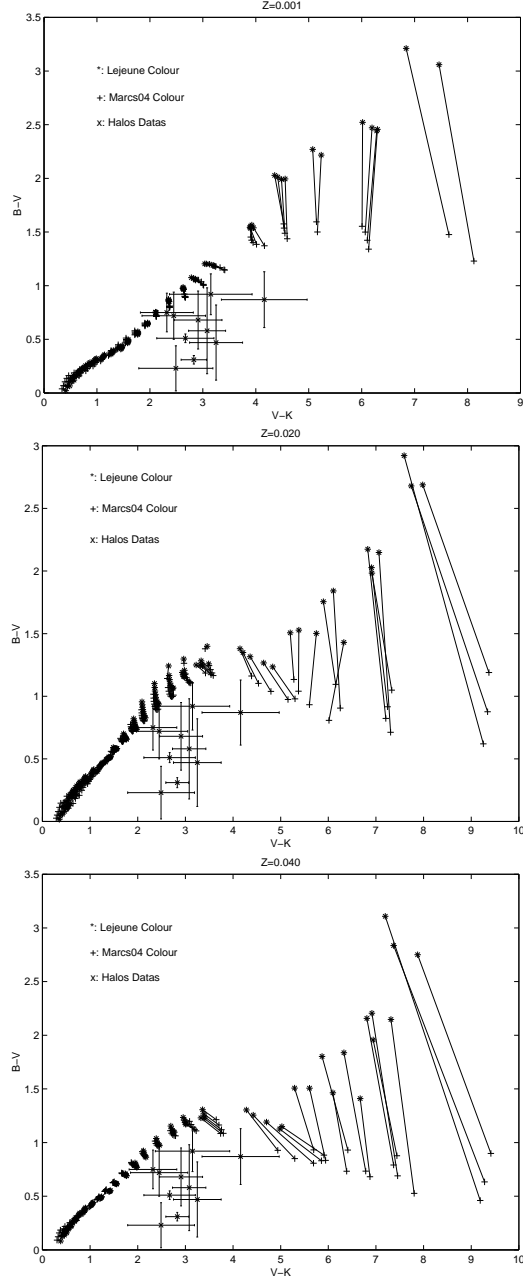


Figure 3. Difference between Lejeune(1998) and MARCS(2004) for $Z = 0.05Z_{\odot}$, $Z = Z_{\odot}$ and $Z = 2Z_{\odot}$. Starred symbols represent the colours computed using Lejeune(1998), crosses are the colours computed using MARCS(2004). The difference in magnitudes become important for the stars with $T = 4000$ (with $V - K \approx 4$ and $B - V \approx 1.5$ for $Z = 0.05Z_{\odot}$ and $V - K \approx 5$ and $B - V \approx 1$ for $Z = 2Z_{\odot}$) and increases for $T < 4000K$. For all the metallicities the greatest difference is in the stars with $T = 2500K$ and $\log(g) = 4.0$.

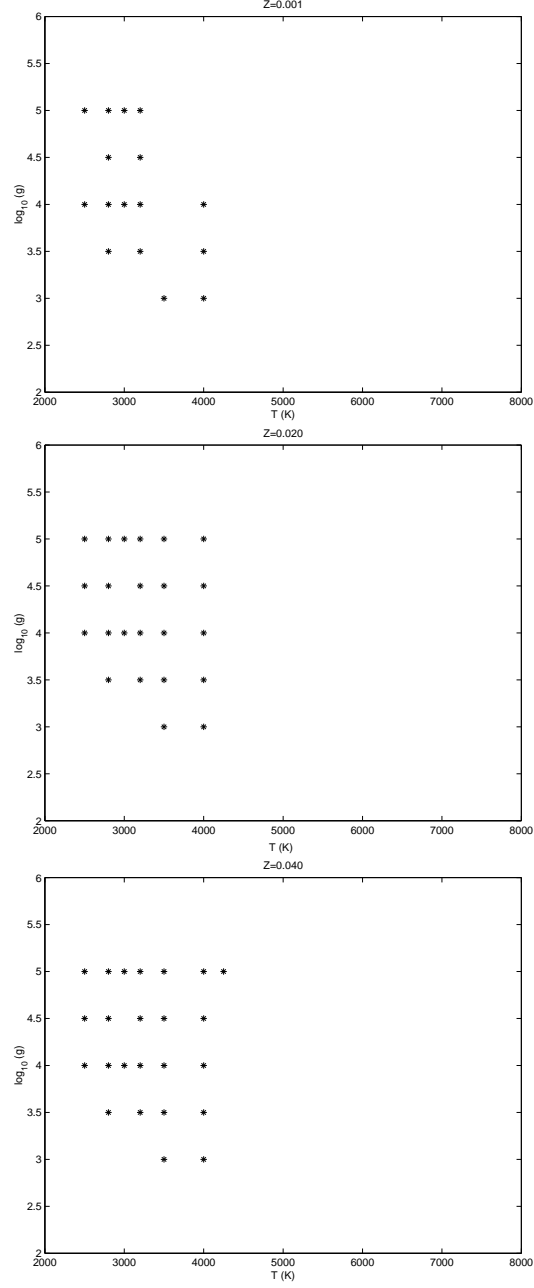


Figure 4. Within the set of stars from MARCS(2004), stars are shown here for whose the difference between Lejeune(1998) and MARCS(2004) colour, in all the directions, bigger of 0.2 magnitudes ($\sqrt{\Delta(V-K)^2 + \Delta(B-V)^2} \geq 0.2$). For all the metallicities the largest difference is in the stars with $T \leq 4000K$.

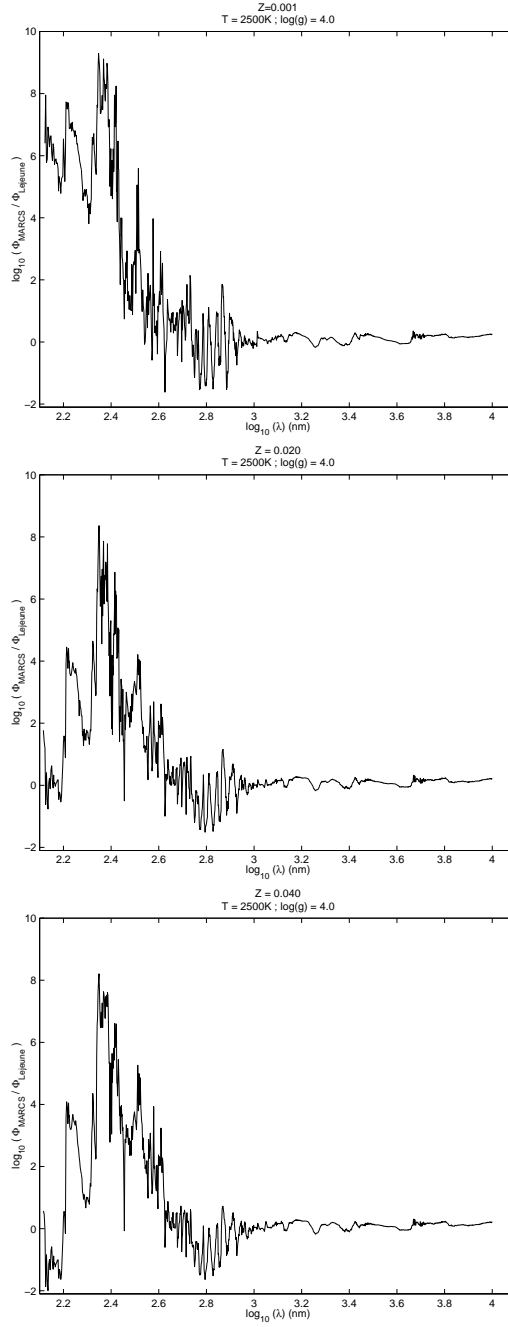


Figure 5. Graph in logarithmic scale of the ratio of Lejeune(1998) and MARCS(2004) spectra for a star with $T = 2500K$ and $\log(g) = 4.0$. The largest difference between the two spectra is in the first part of spectrum. From 125nm to 400nm MARCS(2004) spectrum is up to eight orders of magnitude larger than the Lejeune(1998) spectrum, and from 400nm to 1000nm there are also large differences due to different wavelength positions of peaks.

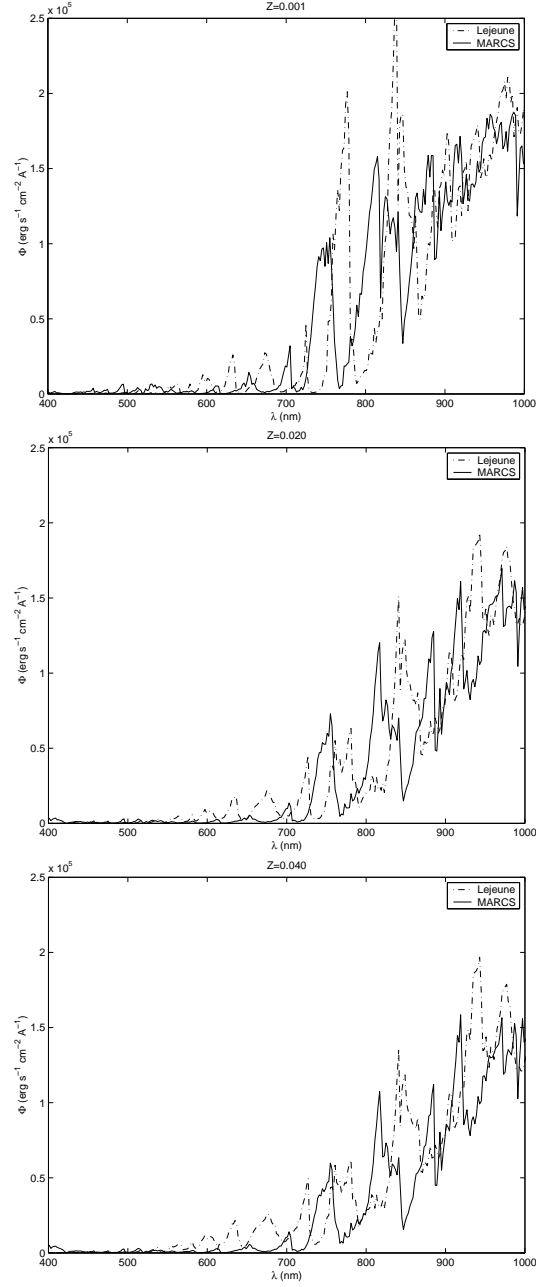


Figure 6. Zoom of the Lejeune(1998) (dash dotted line) and MARCS(2004) (solid line) spectra for a star with $T = 2500K$ and $\log(g) = 4.0$ in the first part of the spectra from 400nm to 1000nm. The different wavelength positions of peaks are evident.

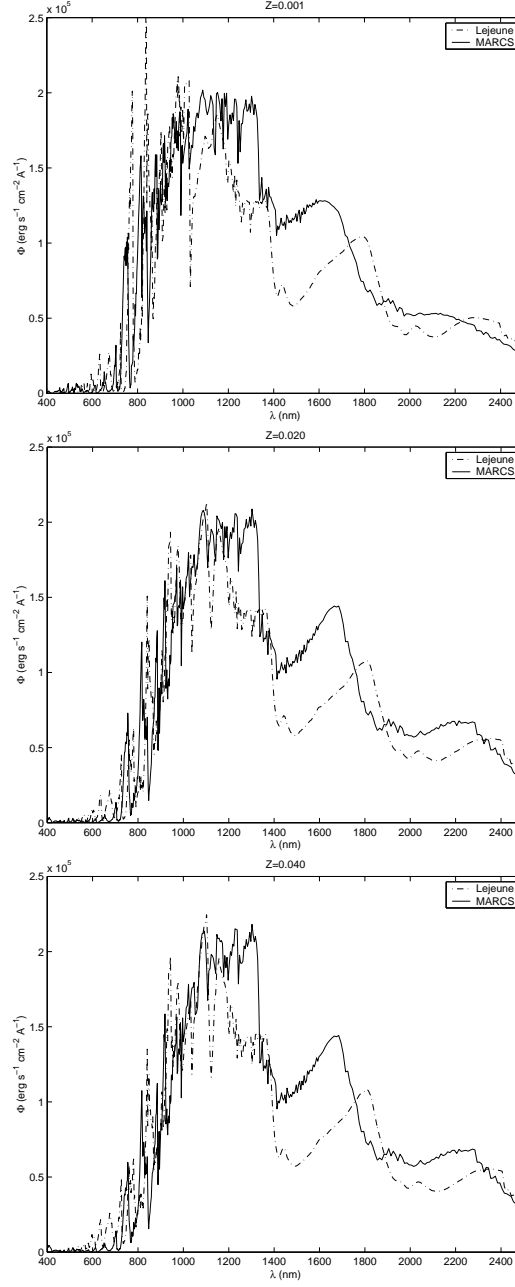


Figure 7. Zoom of the Lejeune(1998) (dash dotted line) and MARCS(2004) (solid line) spectra for a star with $T = 2500K$ and $\log(g) = 4.0$. From 1200nm to 1750nm there is a bigger contribution of flux from MARCS(2004) spectrum which is responsible of the reddening.

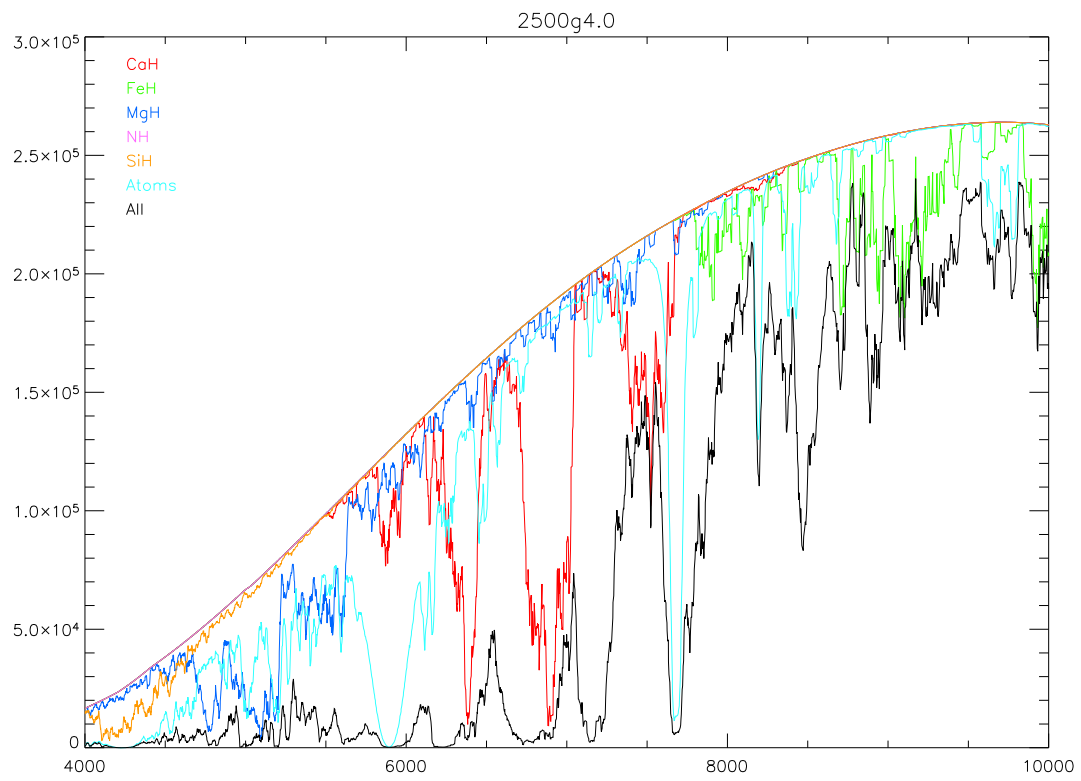
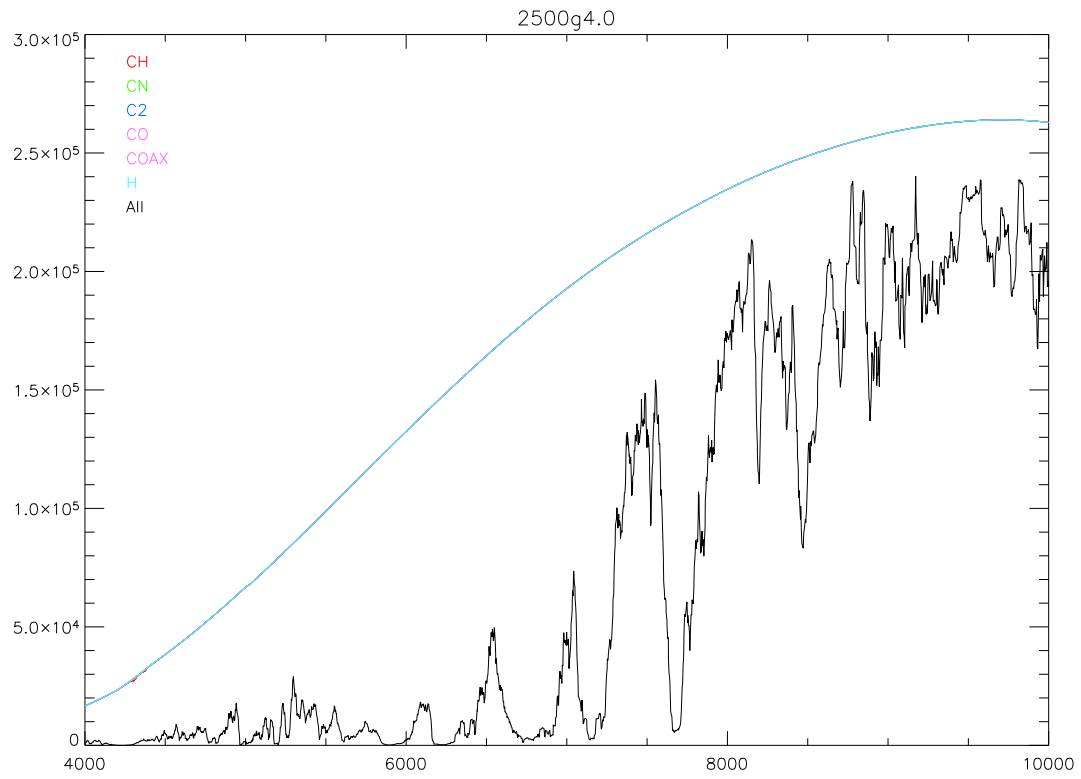


Figure 8. These are the spectra computed by MARCS model for a star with $T = 2500K$ and $\log(g) = 4.0$ since 4000 to 10000 angstrom. We can see the contribution from the different elements.

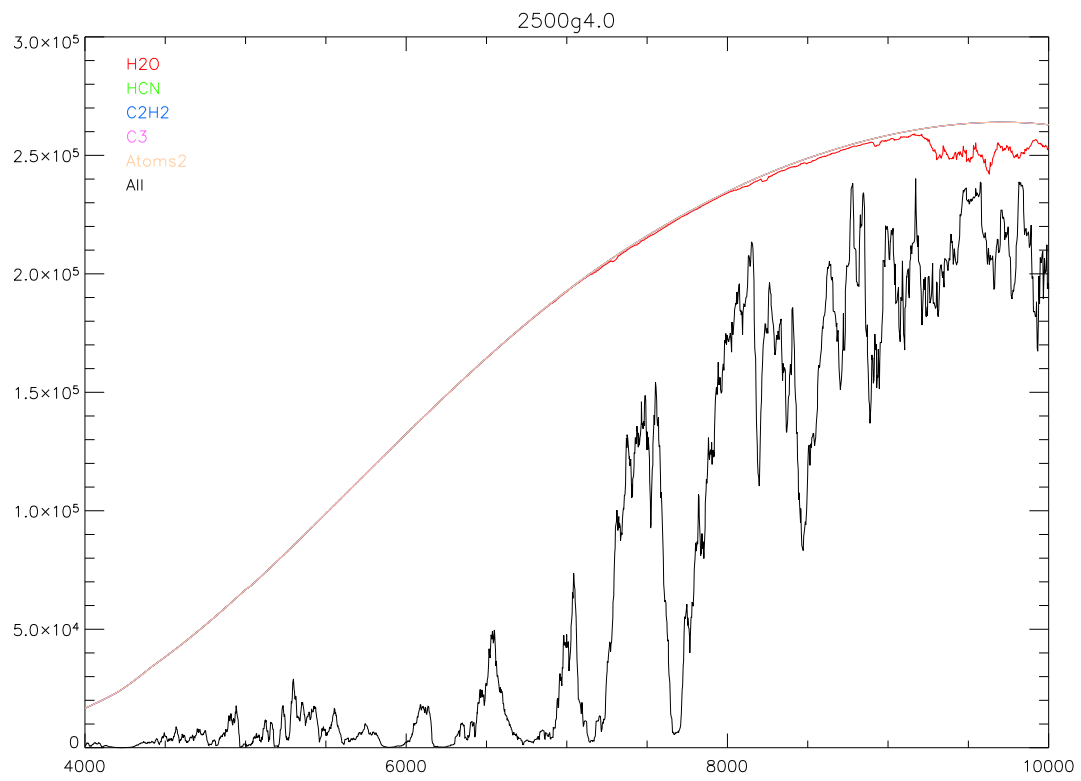
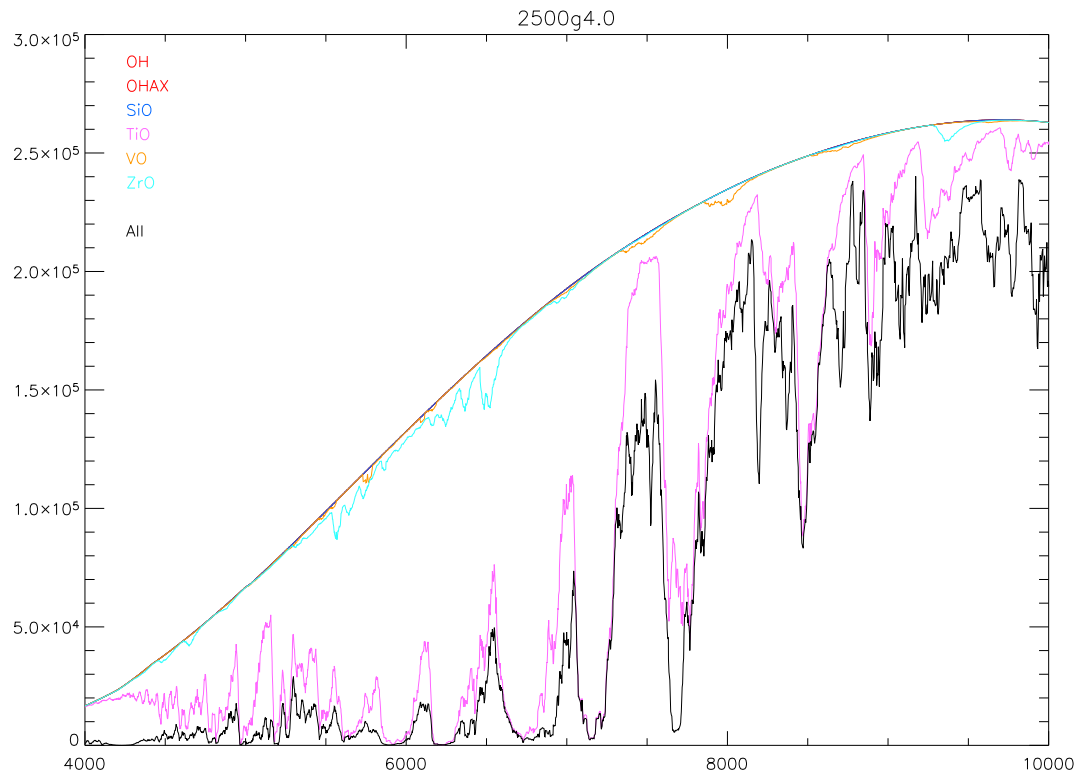


Figure 9. These are the spectra computed by MARCS model for a star with $T = 2500K$ and $\log(g) = 4.0$ since 4000 to 10000 angstrom. We can see the contribution from the different elements.

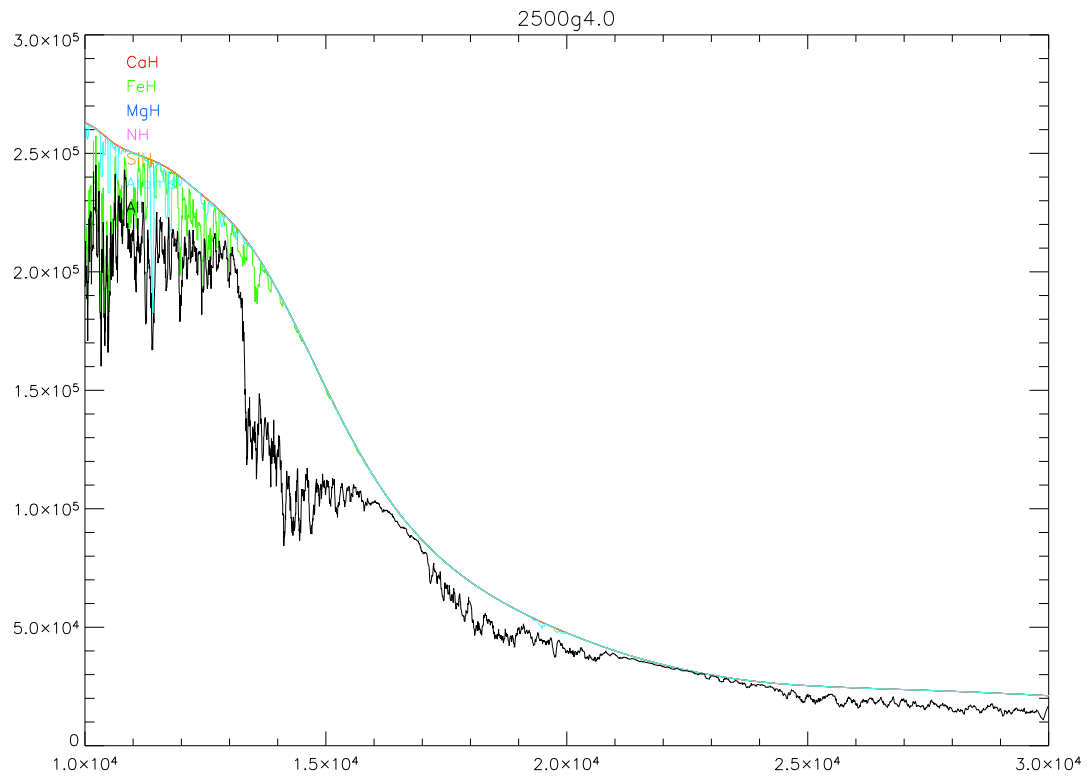
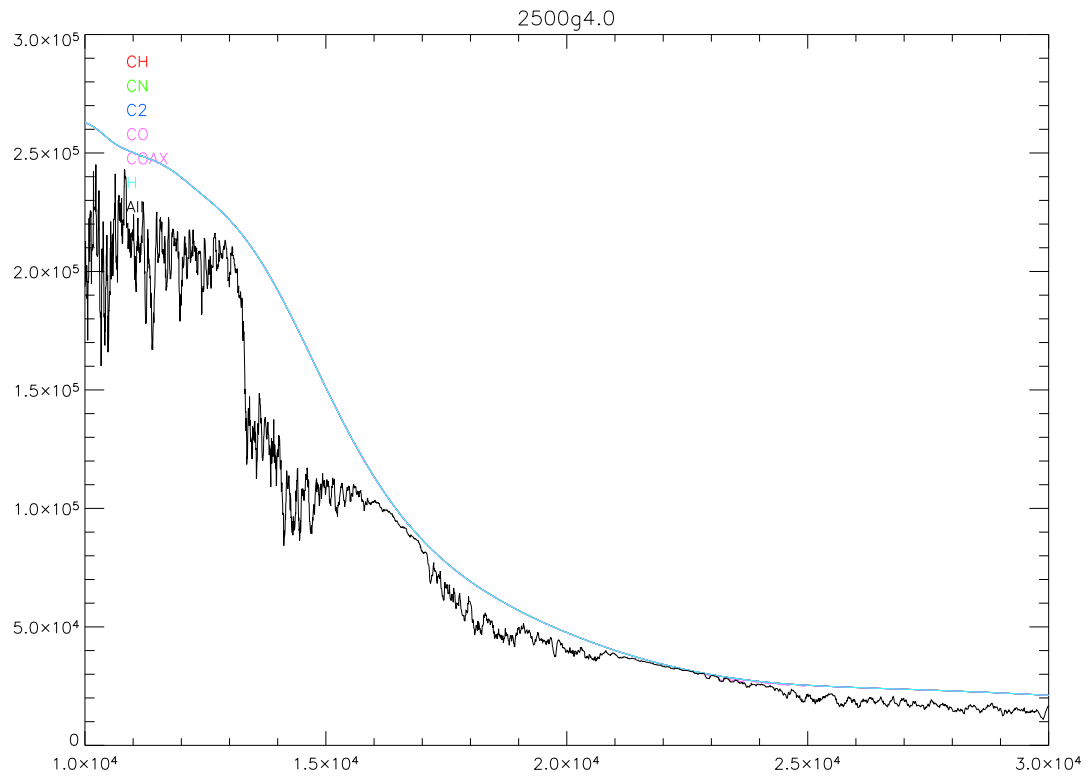


Figure 10. These are the spectra computed by MARCS model for a star with $T = 2500K$ and $\log(g) = 4.0$ since 10000 to 30000 angstrom. We can see the contribution from the different elements.

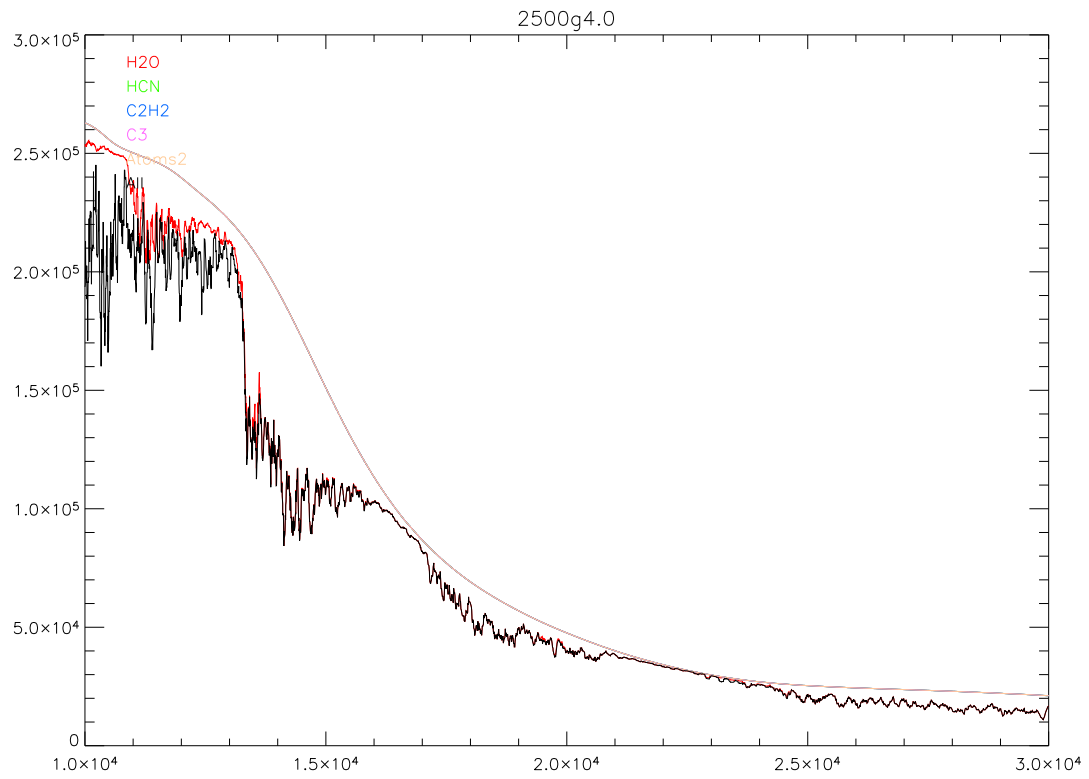
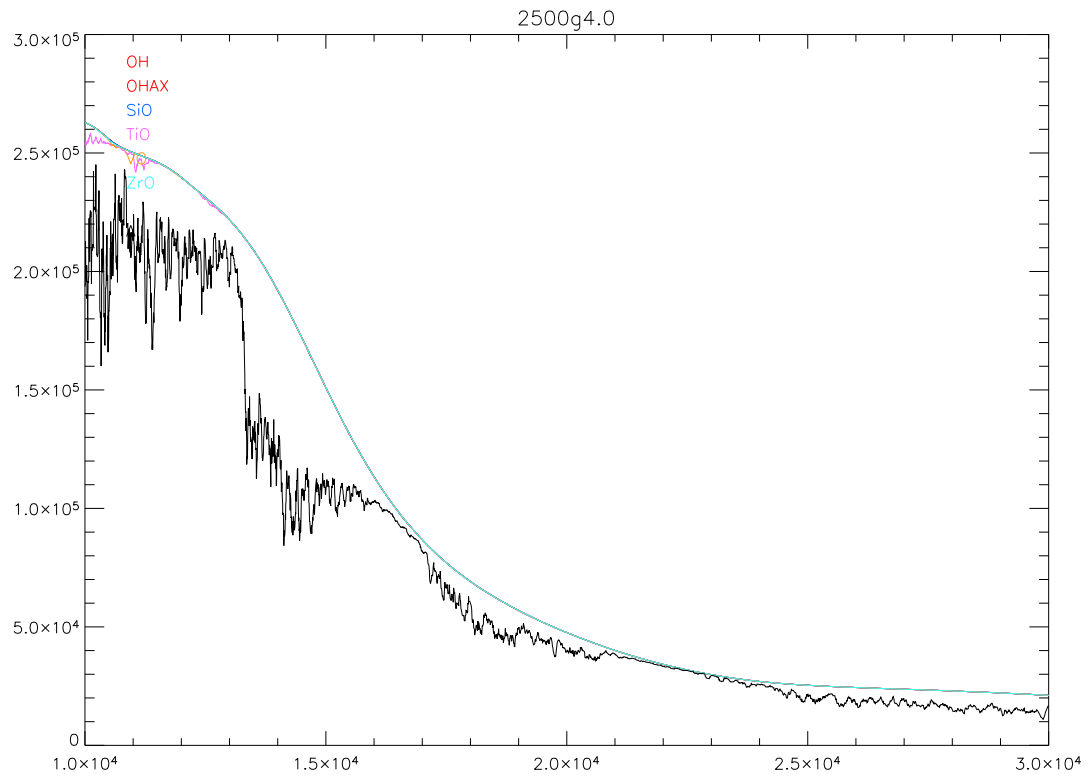


Figure 11. These are the spectra computed by MARCS model for a star with $T = 2500K$ and $\log(g) = 4.0$ since 10000 to 30000 angstrom. We can see the contribution from the different elements.

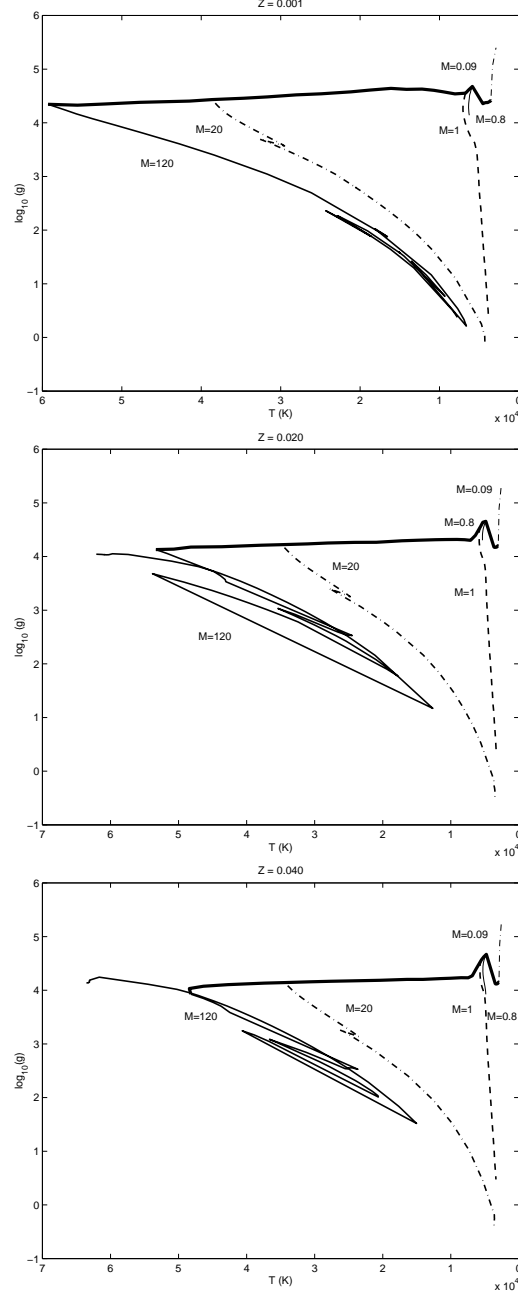


Figure 12. Evolutionary tracks (by the Geneva group) in the $(T, \log(g))$ graph for stars of masses $M = 120M_{\odot}$ (thick solid), $M = 20M_{\odot}$ (thick dash-dotted), $M = M_{\odot}$ (thick dashed), $M = 0.8M_{\odot}$ (thin solid) and $M = 0.09M_{\odot}$ (thin dash-dotted). The main-sequence is the thickest solid line. The stars with $T \leq 4000K$ and $2.5 \leq \log(g) \leq 5.0$ are the low mass stars with $M \leq 0.8M_{\odot}$.

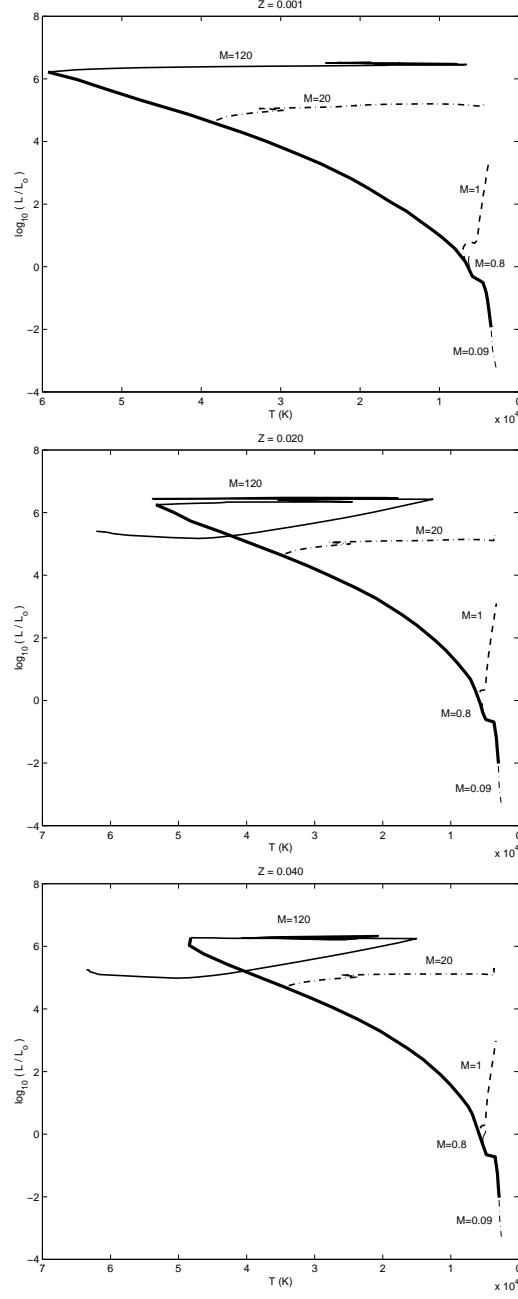


Figure 13. Evolutionary tracks (by the Geneva group) in the $(T, \log(\frac{L}{L_{\odot}}))$ graph for stars of masses $M = 120M_{\odot}$ (thick solid), $M = 20M_{\odot}$ (thick dash-dotted), $M = M_{\odot}$ (thick dashed), $M = 0.8M_{\odot}$ (thin solid) and $M = 0.09M_{\odot}$ (thin dash-dotted). The main-sequence is the thickest solid line. Low mass stars ($M \leq 0.8M_{\odot}$) are the less luminous.

Appendix

Appendix A

```
format long e

%Informations:
file_in2=input('Name of wavelength file:', 's');
file_out1=input('Name of output1 file:', 's');
file_out2=input('Name of output2 file:', 's');

%Creation Of The Character's Matrix:
files='/u55/giovanni/Z=0.001';
names_of_spectra=char(textread([files], '%q'));

%Opening Of Output Files:
fid_out1=fopen( file_out1, 'w');
fid_out2=fopen( file_out2, 'w');

models=0;

%For each file:
for r=1:(size(names_of_spectra,1))
    models=models+1;

    disp(['Processing model: ' num2str(models)])

    file_in1=names_of_spectra(r,:);
    while (file_in1(length(file_in1))== ' ')
        file_in1(length(file_in1))=[];
    end

%Writing On The Output File 2:
    if models==1
        fprintf(fid_out2, 'Spectrum\t\t');
        fprintf(fid_out2, 'Teff\t\t');
        fprintf(fid_out2, 'log(g)\t\t');
        fprintf(fid_out2, 'Z\n');
    end

%Opening Of Input Files:
    fid1=fopen([' /u97/ez/marcs04/z001/' file_in1], 'r');
    fid2=fopen(file_in2, 'r');
```

```

%Reading Original Spectrum File:
dummy=fscanf(fid1,'%20s',1);
Teff=fscanf(fid1,'%g',1);
dummy2=fscanf(fid1,'%20s',1);
logg=fscanf(fid1,'%g',1);
dummy3=fscanf(fid1,'%20s',1);
Z=fscanf(fid1,'%g',1);
raw=fscanf(fid1,'%e %e', [2,inf]);
X=raw(1,:)/10;
Yor=raw(2,:)*10;

%Reading Wavelength File:
Xo=fscanf(fid2,'%f');

%Variables:
Zero=0;
Y=Yor;
A=size(X);
n=1:1220;
o=1:1219;
m=1:(A(2)-1);
l=1:(A(2)-2);
Y(A(2))=[];
Y(1)=[];

Xmed=((X(m+1)+X(m))/2);
Xomed=(Xo(n+1)+Xo(n))/2;
delXmed=Xmed(l+1)-Xmed(l);
delXmedY=delXmed.*Y;
delXomed=Xomed(o+1)-Xomed(o);

i=min(find(Xomed>Xmed(1)));
f=max(find(Xomed<Xmed(A(2)-1)));

%For the last Yo:
Xomed(f)=Xo(f)+(Xo(f)-Xomed(f-1));
delXomed(f-1)=Xomed(f)-Xomed(f-1);

%Operations:
for k=i:f
    a(k)=min(find(Xmed>=Xomed(k)));
end

for p=i:(f-1)
    Yo(p)=(sum(delXmedY(a(p):a(p+1)))/sum(delXmed(a(p):a(p+1))))*10^30;
end

%Conforming of the Vectors:
for g=1:(1224-f)
    Xo(f+1)=[];
end

%Writing Output1 File:

```

```

        fprintf(fid_out1,'%13.4e',models*10^6);
        fprintf(fid_out1,'    ');
        for h=1:(f-1)
            fprintf(fid_out1,'%11.4e',Yo(h));
        end
        for q=1:(1222-f)
            fprintf(fid_out1,'%11.4e',Zero);
        end
        fprintf(fid_out1,'\n');

%Writing on Output2 File:
        fprintf(fid_out2,num2str(models));
        fprintf(fid_out2,'%29.1f',Teff);
        fprintf(fid_out2,'%13.1f',logg);
        fprintf(fid_out2,'%22.3e\n',Z);
        fclose(fid1);
        fclose(fid2);
        clear A delXomed h Teff dummy i dummy2 k Xmed dummy3 l f X Xo...
        Xomed fid1 m Y fid2 n Z file_in1 o Zero p a q delXmed Yo Yor...
        logg raw delXmedY g
    end

%Closing Of Files:
    fclose(fid_out1);
    fclose(fid_out2);
    disp('Finished');

```

Appendix B

```

% Read marcs04's colour:
% -----
file_in1=input('Name of Marcs04 file:', 's');
fid1=fopen(file_in1);
slask1=fscanf(fid1,'%s',15);
rawdata1=fscanf(fid1,'%g',[15,inf]);
fclose(fid1);
rawdata1=rawdata1';
time_new=rawdata1(:,1);
bv_new=rawdata1(:,2);
vbess_new=rawdata1(:,3);
vgunnr_new=rawdata1(:,4);
vgunni_new=rawdata1(:,5);
vj_new=rawdata1(:,6);
vh_new=rawdata1(:,7);
vk_new=rawdata1(:,8);
vl_new=rawdata1(:,9);
v603_new=rawdata1(:,10);
v605_new=rawdata1(:,11);
v606_new=rawdata1(:,12);
v608_new=rawdata1(:,13);
v610_new=rawdata1(:,14);
v_new=rawdata1(:,15);

```



```

% Read lejeune's colour:
% -----
file_in2=input('Name of Lejeune file:', 's');
fid2=fopen(file_in2);
slask2=fscanf(fid2, '%s', 15);
rawdata2=fscanf(fid2, '%g', [15, inf]);
fclose(fid2);
rawdata2=rawdata2';
time_old=rawdata2(:, 1);
bv_old=rawdata2(:, 2);
vbess_old=rawdata2(:, 3);
vgunnr_old=rawdata2(:, 4);
vgunni_old=rawdata2(:, 5);
vj_old=rawdata2(:, 6);
vh_old=rawdata2(:, 7);
vk_old=rawdata2(:, 8);
vl_old=rawdata2(:, 9);
v603_old=rawdata2(:, 10);
v605_old=rawdata2(:, 11);
v606_old=rawdata2(:, 12);
v608_old=rawdata2(:, 13);
v610_old=rawdata2(:, 14);
v_old=rawdata2(:, 15);

%Connections between the two spectra:
%-----
file_in3=input('Name of Legenda marcs04:', 's');
fid3=fopen(file_in3);
slask3=fscanf(fid3, '%20s', 4);
rawdata3=fscanf(fid3, '%g', [4, inf]);
rawdata3=rawdata3';
fclose(fid3);
Teff_new=rawdata3(:, 2);
logg_new=rawdata3(:, 3);

file_in4=input('Name of Legenda Lejeune:', 's');
fid4=fopen(file_in4);
rawdata4=fscanf(fid4, '%g', [3, inf]);
rawdata4=rawdata4';
fclose(fid4);
Teff_old=rawdata4(:, 2);
logg_old=rawdata4(:, 3);

%Halo's data:
%-----
file_in5=input('Name of Halo data:', 's');
fid5=fopen(file_in5);
rawdata5=fscanf(fid4, '%g', [4, inf]);
rawdata5=rawdata5';
fclose(fid5);
bv_halo=rawdata5(:, 1);
bverr_halo=rawdata5(:, 2);
vk_halo=rawdata5(:, 3);

```

```

vkerr_halo=rawdata5(:,4);

%Graphics:
%-----
%(V-K)/(B-V):
%-----
figure(1);
A=size(Teff_new);
for a=1:A(1);
    i=find(Teff_old==Teff_new(a) & logg_old==logg_new(a));
    plot(vk_old(i),bv_old(i),'*k',vk_new(a),bv_new(a),'+k');
    line([vk_new(a) vk_old(i)], [bv_new(a) bv_old(i)]);
    diff(a)=(((bv_new(a)-bv_old(i))^2+(vk_new(a)-vk_old(i))^2)^0.5);
    hold on
end
for b=1:10;
    plot(vk_halo(b),bv_halo(b),'xk');
    hold on
    x=vk_halo(b);
    y=bv_halo(b);

    line([x-vkerr_halo(b),x+vkerr_halo(b)], [y y])
    line([x x], [y-bverr_halo(b),y+bverr_halo(b)])

    line([x-vkerr_halo(b),x-vkerr_halo(b)], [y-0.01,y+0.01])
    line([x+vkerr_halo(b),x+vkerr_halo(b)], [y-0.01,y+0.01])

    line([x-0.02,x+0.02], [y-bverr_halo(b),y-bverr_halo(b)])
    line([x-0.02,x+0.02], [y+bverr_halo(b),y+bverr_halo(b)])
end
title('Z=0.020');
xlabel('V-K');
ylabel('B-V');
text(1,2.75,'*: Lejeune Colour');
text(1,2.5,'+: Marcs04 Colour');
text(1,2.25,'x: Halos Datas');

%Wich stars are the most different:
%-----
figure(2);
stars=find(diff>0.2);
B=size(stars);
for b=1:B(2);
    plot(Teff_new(stars(b)),logg_new(stars(b)),'*k');
    hold on
end
title('Z=0.020');
xlabel('Teff');
ylabel('log(g)');
axis([2000 8000 2 6]);

%Other Colours:
%-----
figure(3);

```

```

for a=1:A(1);
    i=find(Teff_old==Teff_new(a) & logg_old==logg_new(a));
    plot(vh_old(i),vl_old(i),'*k',vh_new(a),vl_new(a),'ok');
    line([vh_new(a) vh_old(i)], [vl_new(a) vl_old(i)]);
    %diff(a)=(((bv_new(a)-bv_old(i))^2+(vk_new(a)-vk_old(i))^2)^0.5);
    hold on
end

```

Appendix C

```

%Comparison:
%-----

%Reading of spectra:
%-----
file_in1=input('Name of Lejeune spectra file:', 's');
file_in2=input('Name of Marcs04 spectra file:', 's');
file_in3=input('Name of wavelenght file:', 's');
file_in4=input('Name of original Marcs04 spectrum file:', 's');
fid1=fopen(file_in1);
fid2=fopen(file_in2);
fid3=fopen(file_in3);
fid4=fopen(file_in4);
rawdata1=fscanf(fid1, '%e', [1221, inf]);
rawdata2=fscanf(fid2, '%e', [1221, inf]);
Xo=fscanf(fid3, '%f');
fclose(fid1);
fclose(fid2);
fclose(fid3);
Xo(1222)=[];
Xo(1222)=[];
Xo(1222)=[];
rawdata1=rawdata1'*10^(-26);
rawdata2=(rawdata2')*10^(-31);
dummy=fscanf(fid4, '%20s', 1);
Teff=fscanf(fid4, '%g', 1);
dummy2=fscanf(fid4, '%20s', 1);
logg=fscanf(fid4, '%g', 1);
dummy3=fscanf(fid4, '%20s', 1);
Z=fscanf(fid4, '%g', 1);
raw=fscanf(fid4, '%e %e', [2, inf]);

%Computing:
%-----
X=raw(1, :)/10;
Yor=raw(2, :);

```